

Lawrence Berkeley National Laboratory

Lawrence Berkeley National Laboratory

Title

Graphene Layer Growth Chemistry: Five-Six-Ring Flip Reaction

Permalink

<https://escholarship.org/uc/item/4jg0108c>

Authors

Whitesides, Russell
Domin, Dominik
Lester Jr., William A.
[et al.](#)

Publication Date

2007-03-24

5th US Combustion Meeting
 Organized by the Western States Section of the Combustion Institute
 and Hosted by the University of California at San Diego
 March 25-28, 2007.

GRAPHENE LAYER GROWTH CHEMISTRY: FIVE-SIX-RING FLIP REACTION

R. Whitesides,¹ D. Domin,² W. A. Lester, Jr.,^{2,3} and M. Frenklach¹

¹ *Department of Mechanical Engineering, University of California, and Environmental Energy Technologies Division, Lawrence Berkeley National Laboratory, Berkeley, CA 94720, USA*

² *Kenneth S. Pitzer Center for Theoretical Chemistry, Department of Chemistry, University of California, Berkeley, CA 94720-1460*

³ *Chemical Sciences Division, Lawrence Berkeley National Laboratory, Berkeley, CA 94720*

A theoretical study revealed a new reaction pathway, in which a fused five and six-membered ring complex on the zigzag edge of a graphene layer isomerizes to reverse its orientation, or “flips,” after activation by a gaseous hydrogen atom. The process is initiated by hydrogen addition to or abstraction from the surface complex. The elementary steps of the migration pathway were analyzed using density-functional theory (DFT) calculations to examine the region of the potential energy surface associated with the pathway. The DFT calculations were performed on substrates modeled by the zigzag edges of tetracene and pentacene. Rate constants for the flip reaction were obtained by the solution of energy master equation utilizing the DFT energies, frequencies, and geometries. The results indicate that this reaction pathway is competitive with other pathways important to the edge evolution of aromatic species in high temperature environments.

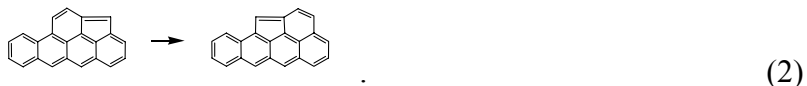
1. Introduction

Soot production as a by-product of hydrocarbon combustion remains an important engineering problem. Surface growth of soot particles is a critical part of modeling soot producing systems, as most of the soot mass is acquired via gas-surface reactions. Our goal is to gain fundamental understanding of evolution of soot particles, including their atomistic structures and surfaces. In recent studies [1], a new phenomenon was discovered—migration of five-membered rings along the zigzag edge of the evolving graphene layer. This phenomenon of migration alters significantly the framework for surface chemistry of graphene layer, and introduces a large number of possible elementary reaction steps that could take place on an evolving surface. One such example is the “collision” of migrating rings examined in our prior study [2], which results in the following transformation

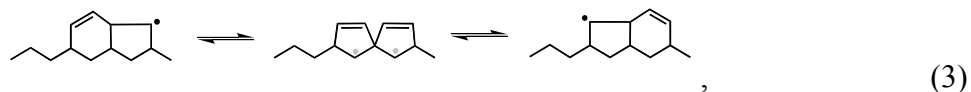


Reaction rates of this pathway were found to be comparable to those of the migration reaction, while the latter was reported to be one of the fastest reaction steps in zigzag-edge graphene chemistry [1].

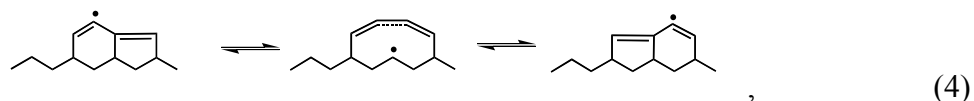
In considering the fate of the product of reaction (1), we identified a new reaction pathway, re-orientation, or “flipping”, of the surface complex



The flip rearrangement is initiated by hydrogen-atom addition,



or hydrogen-atom abstraction,



from the initial surface molecule. Here we present results of a quantitative study of these two reaction channels.

2. Computational Methods

Density functional theory (DFT) was used to calculate the molecular and energetic parameters of all stable species and transition states involved in the ring flip reaction sequences. The substrates for the calculations were modeled by the zigzag edges of tetracene and pentacene. Geometry optimizations were performed with the B3LYP hybrid functional [3] and the 6-311G(d,p) basis set. Previous studies have shown energetic predictions of B3LYP calculations at the 6-311G(d,p) level to be in good agreement with experimental and high-level ab initio results for stable species [4-6]. The energies of transition states predicted by this method, however, are often underestimated by about 5 kcal mol⁻¹ [7,8]. This shortcoming lessens the accuracy of rate constants derived from the calculated energetics yet allows for an order-of-magnitude analysis.

Force calculations were performed at each predicted stationary point to confirm the point to be an energetic minimum (no imaginary frequencies) or a saddle point (one imaginary frequency). Transition states were confirmed to connect the reactant and product stable species by visual inspection of normal modes corresponding to the imaginary frequencies calculated at the B3LYP/6-311G(d,p) level. Zero point energies were determined from the force calculations and scaled by a factor of 0.9668 [9]. All calculations were performed using the Gaussian 03 suite of codes [10] on an Intel Xeon cluster.

Chemical activation rate constants for the addition reaction pathway and transition-state-theory rate constants for the abstraction pathway were determined using version 2.06 of the MultiWell suite of codes [11,12]. MultiWell employs a stochastic approach to solution of the master equations for energy transfer in unimolecular reaction systems [11,13]. Microcanonical rate constants for the elementary reactions of these models were calculated with MultiWell at the RRKM level of theory.

The key inputs to MultiWell—reaction barriers, frequencies, and moments of inertia—were assigned from the DFT calculations at the B3LYP/6-311G(d,p) level of the present study. Following Gilbert and Smith [14] the real frequencies below 150 cm⁻¹ were examined by

graphically visualizing the associated normal mode vibrations to identify internal rotational modes. No species examined herein were found to exhibit internal rotation.

The sums and densities of states for intermediate species and transition states were determined by exact count with a grain size of 10 cm^{-1} , maximum energy of $300,000\text{ cm}^{-1}$, and the dividing level between the high and low energy regimes set at 2500 cm^{-1} . Lennard-Jones parameters for the reactants and intermediates were taken from an empirical correlation [15]. Argon was chosen as the bath gas collider. The collisional energy transfer was treated by the exponential-down model with $\langle\Delta E_{\text{down}}\rangle = 260\text{ cm}^{-1}$ based on the data of Hippler et al. [16].

MultiWell simulations were performed for temperatures ranging from 1500 to 2500 K and pressures ranging from 0.1 to 10 atm. The numerical runs were carried out for reaction times ranging from 1×10^{-8} to 1×10^{-6} s. For each set of conditions, between 10^6 and 10^8 stochastic trials were performed to maintain statistical error in the species fractions of less than 4%.

3. Results and discussion

The combined potential energy surface for the two reaction pathways is shown in Fig. 1. The upper, higher-energy, pathway is initiated by hydrogen atom abstraction, and the lower-energy pathway is initiated by hydrogen atom addition. The numbering scheme for the species is consistent with the previously published collision pathway [2]. The split radical dot shown on species **20** indicates that the species has a single delocalized unpaired electron.

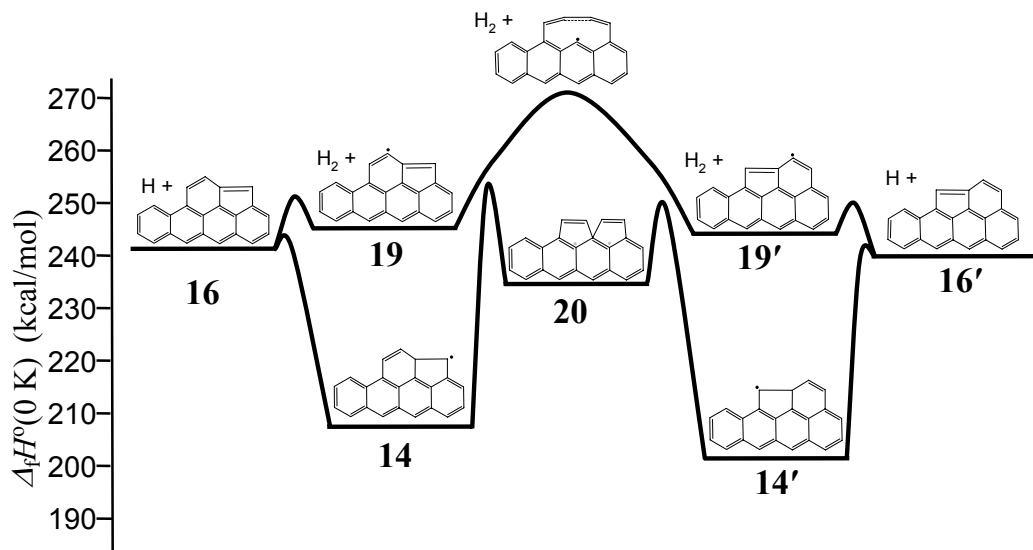


Figure 1: Potential energy diagram for the flip reaction calculated at the B3LYP/6-311G(d,p) level of quantum theory

Table 1 reports computed energies, comparing the results obtained with two substrates: tetracene, as shown in Fig. 1, and pentacene, with an additional ring added to the right-hand side of the molecules as they are depicted in Fig. 1. The results reported in Table 1 indicate that the critical barriers along both pathways, TS14-20 and TS19-19', are reduced by 7 and 5 kcal mol⁻¹, respectively, with the additional substrate ring. Species **14** and **20** on the addition pathway

became more stable by enlarging the substrate, while the energy of species **19** on the abstraction pathway was changed only slightly.

Table 1: Energetics of flip reaction (kcal mol⁻¹ relative to reactant)

Species	Tetracene Substrate	Pentacene Substrate
16	0.0	0.0
14	-33.2	-39.9
14'	-39.9	-39.9
19	4.2	3.3
19'	2.9	3.3
20	-6.8	-10.8
16'	-1.6	0.0
TS16-14	2.9	<i>a</i>
TS14-20	13.5	6.3
TS20-14'	10.4	6.3
TS14'-16'	1.2	<i>a</i>
TS16-19	9.9	<i>a</i>
TS19-19'	29.5	24.4
TS19'-16'	8.6	<i>a</i>

^aThe quantum chemical calculations were not fully converged at the time of this writing.

The optimized geometry of species **20** is shown in Fig. 2. The relatively high stability of this molecule with respect to other species in the reaction network was a surprising result of the DFT calculations. Constrained optimization and energy calculations were performed with an idealized planar aromatic substrate to determine the influence of a stiffer substrate on the energetics of this species. For these constrained calculations, the perimeter substrate carbon atoms labeled 1 through 11 in Fig. 2 were held fixed to the positions they have in tetracene. The difference in the B3LYP/6-311G(d,p) single point energies of species **16** and **20** without geometric constraint is 12 kcal mol⁻¹ and with constraint is 10 kcal mol⁻¹. This small change in energy indicates that the reaction pathway through species **20** will remain energetically feasible in more constrained environments, such as on larger substrates which cannot bend as readily as the tetracene molecule.

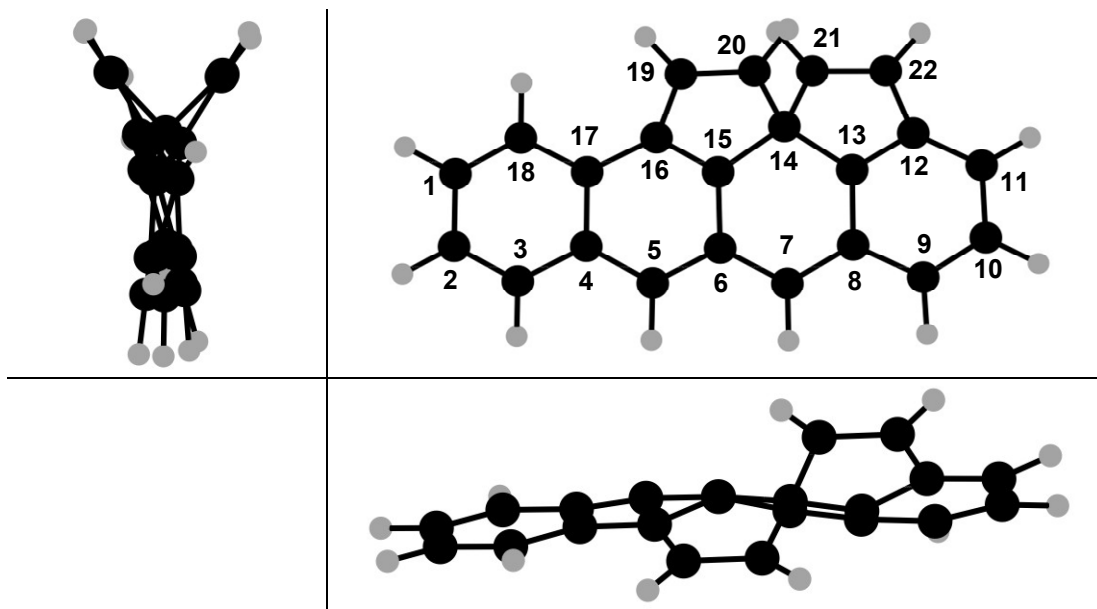


Figure 2: Species 20 optimized at the B3LYP/6-311G(d,p) level of theory

The computed reaction rates for the flip reaction are displayed in Fig. 4.

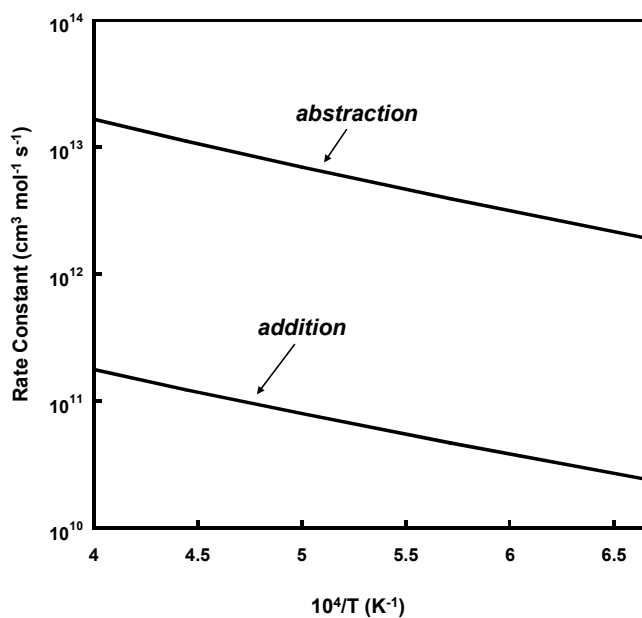
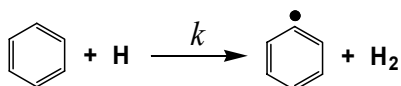
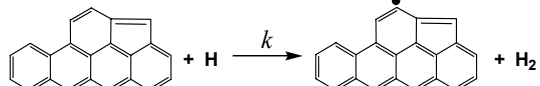


Figure 4: Flip rate constants for the addition and abstraction pathways calculated with the quantum chemical information from the tetracene substrate system at a pressure of 1 atm.

The results for the addition channel shown in Fig. 4 were obtained at a pressure of 1 atm. Calculations at 0.1 and 10 atm showed less than 4 % difference from the 1 atm results, at the level of the stochastic error (see Sec. 2), indicating that the reactions are at their high-pressure limit. For the abstraction pathway, the overall reaction was modeled as a three step process:

(1) bimolecular reaction forming **19** by hydrogen abstraction from **16**, (2) unimolecular transformation of the radical intermediate, $\mathbf{19} \rightarrow \mathbf{19}'$, and (3) bimolecular reaction of $\mathbf{19}'$ with H_2 to form $\mathbf{16}'$. The rate of the unimolecular transformation, step 2, is found to be on the order of 10^{10} – 10^{11} s^{-1} between 1500 and 2500 K. Considering that the rate of abstraction, step 1, is on the order of 10^{12} – $10^{13} [\text{H}] \text{ cm}^3 \text{ mol}^{-1} \text{ s}^{-1}$ for the same temperature range, the abstraction step will be rate determining even for very large mole fractions of hydrogen atom. As a result, fast interconversion will create partial equilibrium between species **19** and $\mathbf{19}'$. The radical can then react with H_2 either back to the initial species, **16**, or forward to the flipped species, $\mathbf{16}'$, with equal probability (for a symmetric substrate). Therefore, the rate for the overall flip abstraction pathway can be assumed to be half of the hydrogen abstraction rate. In Table 2, we compare the equilibrium constant and rate coefficient of the H abstraction reaction calculated in the present work with that of hydrogen abstraction from benzene [17].

Table 2: Comparison of hydrogen-abstraction reactions for benzene [17] and species 16 (flip reactant) calculated by TST with quantum chemical information from the tetracene substrate system

						
Temperature (K)	K_{eq}	$k \text{ (cm}^3 \text{ mol}^{-1} \text{ s}^{-1}\text{)}$	K_{eq}	$k \text{ (cm}^3 \text{ mol}^{-1} \text{ s}^{-1}\text{)}$		
1500	1.29	1.95×10^{11}	3.06	3.80×10^{12}		
1750	1.66	4.20×10^{11}	3.64	7.85×10^{12}		
2000	1.97	7.46×10^{11}	4.07	1.39×10^{13}		
2250	2.23	1.17×10^{12}	4.38	2.23×10^{13}		
2500	2.44	1.67×10^{12}	4.58	3.31×10^{13}		

The total rate for the flip transformation is displayed in Fig. 5 and compared with the previously reported rates of graphene edge ring migration and collision reactions [2]. Inspection of results reported in Fig. 5 indicates that the rate of the combined flip reaction is on the same order of magnitude and faster than those for the collision and migration reactions. This fast reaction rate suggests that in evolving graphene layers flipping of the complex formed by the collision reaction should occur frequently.

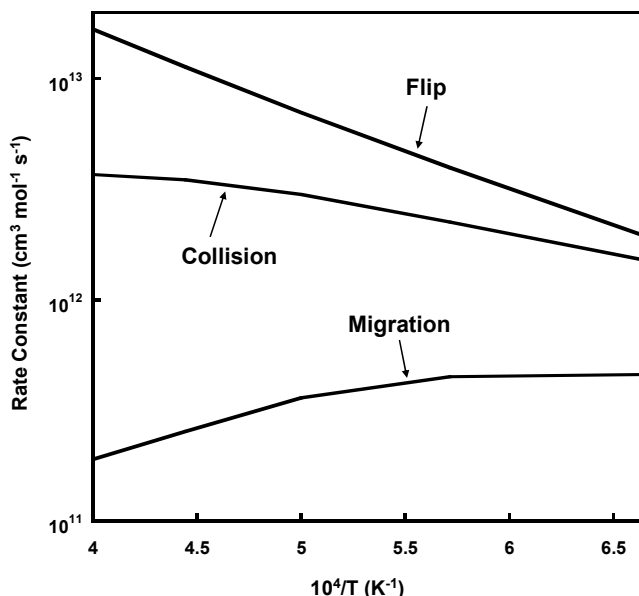


Figure 5: Comparison of rate constants for total flip reaction, calculated at a pressure of 1 atm, with rate constants for the collision and migration reactions [2].

4. Conclusions

The analysis of the proposed flip reaction indicates that it occurs with rates comparable to and exceeding those of migration and collision reactions, and the latter suggested to play an important role in graphene zigzag edge chemistry in flame environments [2]. The new reaction adds a possibly important step in graphene layer growth, thus suggesting an even more complex network of elementary reaction steps than suspected earlier.

Acknowledgments

Russell Whitesides, William A. Lester, Jr., and Michael Frenklach were supported by the Director, Office of Energy Research, Office of Basic Energy Sciences, Chemical Sciences, Geosciences and Biosciences Division of the US Department of Energy, under Contract No. DE-AC03-76F00098. Dominik Domin was supported by the CREST Program of the National Science Foundation under Grant No. HRD-0318519.

References

- [1] M. Frenklach, C.A. Schuetz, J. Ping, *Proc. Combust. Inst.* 30 (2005) 1389-1396.
- [2] R. Whitesides, A.C. Kollias, D. Domin, W.A. Lester, Jr., M. Frenklach, *Proc. Combust. Inst.* 31 (2007) 539-546.
- [3] A.D. Becke, *J. Chem. Phys.* 98 (1993) 5648-5652.
- [4] N.W. Moriarty, N.J. Brown, M. Frenklach, *J. Phys. Chem. A* 103 (1999) 7127-7135.
- [5] M.R. Nimlos, J. Filley, J.T. McKinnon, *J. Phys. Chem. A* 109 (2005) 9896-9903.
- [6] J. Cioslowski, P. Piskorz, D. Moncrieff, *J. Am. Chem. Soc.* 120 (1998) 1695-1700.
- [7] J.L. Durant, *Chem. Phys. Lett.* 256 (1996) 595-602.
- [8] J.P.A. Heuts, R.G. Gilbert, L. Radom, *J. Phys. Chem.* 100 (1996) 18997-19006.

- [9] R.D. Johnson, III (Ed.) *NIST Computational Chemistry Comparison and Benchmark Database*. National Institute of Standards and Technology, Aug 2005; <http://srdata.nist.gov/cccbdb>.
- [10] M.J. Frisch, *et al.*, Gaussian 03, Revision C.02, Gaussian, Inc., Wallingford, CT, 2004;
- [11] J.R. Barker, *Int. J. Chem. Kinet.* 33 (2001) 232-245.
- [12] J.R. Barker, N.F. Ortiz, J.M. Preses, L.L. Lohr, A. Maranzana, P.J. Stimac, MultiWell, 2.06, 2007; <http://aoss.engin.umich.edu/multiwell/>.
- [13] J.R. Barker, L.M. Yoder, K.D. King, *J. Phys. Chem. A* 105 (2001) 796-809.
- [14] R.G. Gilbert, S.C. Smith, *Theory of Unimolecular and Recombination Reactions*. Blackwell-Scientific, Oxford, 1990.
- [15] H. Wang, M. Frenklach, *Combust. Flame* 96 (1994) 163-170.
- [16] H. Hippler, J. Troe, H.J. Wendelken, *J. Chem. Phys.* 78 (1983) 6709-6717.
- [17] J.H. Kiefer, L.J. Mizerka, M.R. Patel, H.C. Wei, *J. Phys. Chem.* 89 (1985) 2013-2019.